

## Facilitation of polymer looping and giant polymer diffusivity in crowded solutions of active particles

This content has been downloaded from IOPscience. Please scroll down to see the full text.

2015 New J. Phys. 17 113008

(<http://iopscience.iop.org/1367-2630/17/11/113008>)

View [the table of contents for this issue](#), or go to the [journal homepage](#) for more

Download details:

IP Address: 141.89.176.205

This content was downloaded on 29/10/2015 at 11:08

Please note that [terms and conditions apply](#).



## PAPER

## Facilitation of polymer looping and giant polymer diffusivity in crowded solutions of active particles

## OPEN ACCESS

RECEIVED  
13 July 2015REVISED  
3 September 2015ACCEPTED FOR PUBLICATION  
30 September 2015PUBLISHED  
28 October 2015

Content from this work  
may be used under the  
terms of the [Creative  
Commons Attribution 3.0  
licence](#).

Any further distribution of  
this work must maintain  
attribution to the  
author(s) and the title of  
the work, journal citation  
and DOI.

Jaehoh Shin<sup>1,2,5</sup>, Andrey G Cherstvy<sup>1</sup>, Won Kyu Kim<sup>3</sup> and Ralf Metzler<sup>1,4</sup><sup>1</sup> Institute for Physics & Astronomy, University of Potsdam, D-14476 Potsdam-Golm, Germany<sup>2</sup> Max Planck Institute for the Physics of Complex Systems, D-01187 Dresden, Germany<sup>3</sup> Fachbereich Physik, Freie Universität Berlin, D-14195 Berlin, Germany<sup>4</sup> Department of Physics, Tampere University of Technology, 33101 Tampere, Finland<sup>5</sup> Author to whom any correspondence should be addressed.E-mail: [jshin@pks.mpg.de](mailto:jshin@pks.mpg.de)**Keywords:** diffusion, active transport, polymersSupplementary material for this article is available [online](#)

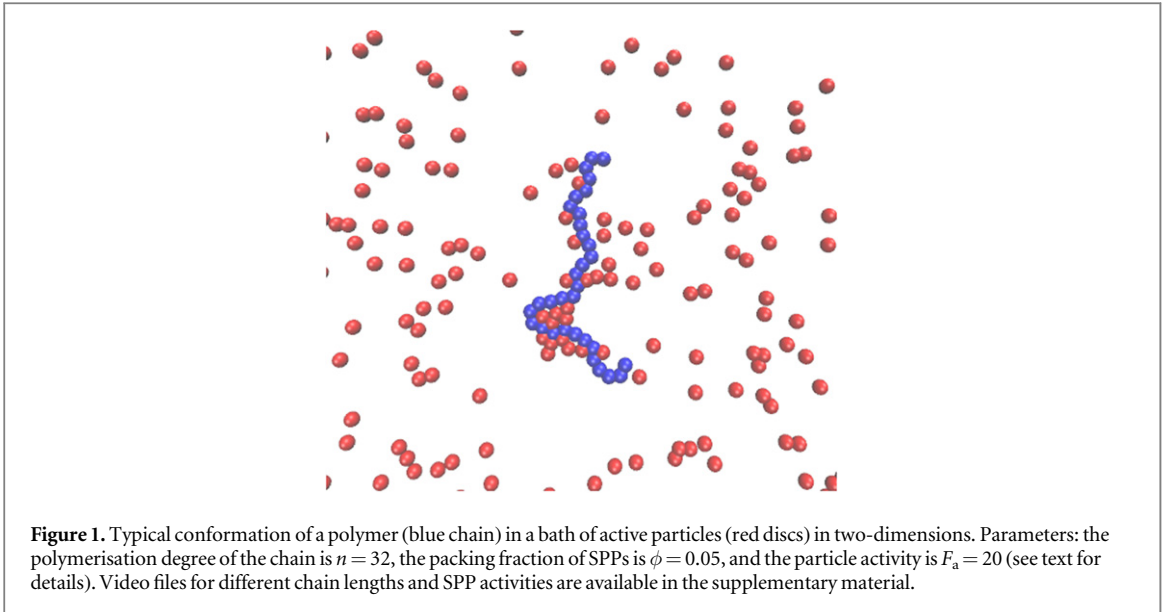
### Abstract

We study the dynamics of polymer chains in a bath of self-propelled particles (SPP) by extensive Langevin dynamics simulations in a two-dimensional model system. Specifically, we analyse the polymer looping properties versus the SPP activity and investigate how the presence of the active particles alters the chain conformational statistics. We find that SPPs tend to extend flexible polymer chains, while they rather compactify stiffer semiflexible polymers, in agreement with previous results. Here we show that higher activities of SPPs yield a higher effective temperature of the bath and thus facilitate the looping kinetics of a passive polymer chain. We explicitly compute the looping probability and looping time in a wide range of the model parameters. We also analyse the motion of a monomeric tracer particle and the polymer's centre of mass in the presence of the active particles in terms of the time averaged mean squared displacement, revealing a giant diffusivity enhancement for the polymer chain via SPP pooling. Our results are applicable to rationalising the dimensions and looping kinetics of biopolymers at constantly fluctuating and often actively driven conditions inside biological cells or in suspensions of active colloidal particles or bacteria cells.

### 1. Introduction

Active motion is a necessary prerequisite for living systems to maintain a number of vital processes, including materials transport inside cells and the foraging dynamics of mobile organisms [1, 2]. The length scales associated with active motion processes span several orders of magnitude and range from the nanoscopic motion of cellular molecular motors [3] essential to move larger cargo in the crowded environment of cells [4], over the microscopic motion of bacteria cells and microswimmers [5, 6], to the macroscopic motion patterns of higher animals and humans [7]. In particular, artificial Janus colloids are propelled by diffusiophoretic or thermophoretic forces [8–10]. Active motion also enhances the speed and precision of signalling and cargo transport in biological cells [11] and allows efficient search of sparse targets for large organisms [12].

A somewhat different question is how passive particles are influenced by an active environment. Tracking the motion of tracer particles immersed in baths of active bacteria [13, 14] and swimming eukaryotic cells [15] one typically observes an enhanced effective tracer mobility, and the active environment may lead to exponential tails of the displacement distribution of the particles [15, 16]. Passive particles may also become enslaved to the motion of motor-cargo complexes due to cytoplasmic drag [17]. When micron sized colloids are immersed in baths with smaller particles, short ranged attractive depletion forces of entropic origin emerge [18]. However, the same colloids in a bath of self-propelled particles (SPPs) may experience long ranged attractive or repulsive forces depending on the SPP characteristics [19]. For instance, by tuning the concentration of SPPs the forces between two plates can be controlled [20], in particular due to accumulation of active particles near the walls



[21]. Some attractive interactions in suspensions of active particles were shown to promote—in contrast to hydrodynamic interactions which rather suppress—the motility-induced phase separation in the system, see e.g. [22].

Here we want to focus on the properties of polymer chains in an active liquid, see [23–25]. It is known that when a polymer chain is immersed into an SPP bath its extension can change non-monotonically with the activity  $F_a$  of active particles due to competing effects of active forces and chain elasticity [26, 27]. We study here the extent to which the activity of SPPs alters the *internal* motion of a polymer chain, specifically, how its end loop formation kinetics becomes affected. Polymer looping or reactions of the chain ends is a fundamental process governing numerous biological functions [28, 29]. Protein mediated DNA looping, for instance, is involved in gene regulatory processes [30–32], or DNA and RNA constructs may be used as molecular beacon sensors [33].

We quantify the behaviour of a polymer chain immersed in a bath of SPPs in two dimensions, see the snapshot of our system in figure 1. We find that the activity  $F_a$  of SPPs differently affects the chain conformations depending on the chain bending stiffness  $\kappa$ . Active particles significantly enhance the looping kinetics as well as give rise to a giant diffusivity of the centre of mass motion of the chain due to SPP pooling in typical *parachute* like polymer configurations. We analyse the diffusion of a monomeric tracer particle, which shows superdiffusive motion on short time scales and Brownian behaviour with enhanced diffusivity in the long time limit. In [26, 27] a similar system was considered, the main focus being on equilibrium polymer properties such as the gyration radius of the chain. Below we systematically analyse dynamic properties of flexible and semiflexible polymer chains. Our results demonstrate that the equilibrium and dynamic properties of SPPs-driven polymers are to be considered on the same footing.

This paper is organised as follows. We introduce our model and the simulations methods in section 2. In section 3.1 we examine the equilibrium properties of the polymer chain. Section 3.2 presents the main results regarding the polymer looping properties. In section 3.3 we study the dynamical effects of SPPs on the tracer diffusion, in order to understand its implications on the enhancement of the polymer looping kinetics. We summarize our results and discuss their possible applications in section 4.

## 2. Model and methods

To study the dynamics of a polymer chain immersed in a bath of SPPs in two dimensions, we employ coarse grained computer simulations. The polymer chain is modelled as a bead spring chain consisting of  $n$  monomers of diameter  $\sigma$ , connected by harmonic springs with the potential

$$U_s = \frac{k}{2} \sum_{i=2}^n (|\mathbf{r}_i - \mathbf{r}_{i-1}| - l_0)^2. \quad (1)$$

Here  $k$  is the spring constant and  $l_0$  is the equilibrium bond length. The self avoidance of the chain monomers is modelled by the repulsive part of the Lennard–Jones (LJ) potential (the so called Weeks–Chandler–Andersen or WCA potential)

$$U_{\text{LJ}}(r) = 4\epsilon \left[ \left( \frac{\sigma}{r} \right)^{12} - \left( \frac{\sigma}{r} \right)^6 \right] + C(r_{\text{cut}}). \quad (2)$$

for  $r \leq r_{\text{cut}}$ , where  $r_{\text{cut}}$  is a cutoff distance. Moreover  $C(r_{\text{cut}})$  is a constant that ensures that  $U_{\text{LJ}}(r) = 0$  for separations  $r > r_{\text{cut}}$ , and  $r$  is the inter-monomer distance. The potential strength is denoted by  $\epsilon$ . With the standard choice  $r_{\text{cut}} = 2^{1/6}\sigma$  for the cutoff length the potential is purely repulsive. In what follows, we measure the length in units of  $\sigma$  and the energy in units of the thermal energy  $k_{\text{B}}T$ , where  $k_{\text{B}}$  is the Boltzmann constant and  $T$  is the absolute temperature. Below we set the model parameters to  $\sigma = 1$ ,  $l_0 = 1.12$ ,  $k = 10^3$ , and  $\epsilon = 1$ .

The bending energy of the chain is given by

$$U_{\text{b}} = \frac{\kappa}{2} \sum_{i=2}^{n-1} (\mathbf{r}_{i-1} - 2\mathbf{r}_i + \mathbf{r}_{i+1})^2, \quad (3)$$

where  $\kappa$  is the bending stiffness (measured below in units of the thermal energy). For a given value of  $\kappa$ , the chain persistence length is  $l_{\text{p}} \sim 2\kappa l_0^3 / (k_{\text{B}}T)$  in two-dimensions. The end monomers are subject to short ranged attractive interactions mimicking the biologically relevant situation that closed structures are energetically profitable, as known for specific DNA looping [30] or closed single stranded DNA (hairpins) [34]. We include the attractive interactions via the LJ potential in equation (2) but with a larger cutoff distance and attraction strength  $\epsilon_{\text{s}}$ , namely

$$U_{\text{att}}(r) = U_{\text{LJ}}(r, \epsilon_{\text{s}}) \quad (4)$$

and  $r_{\text{cut}} = 2\sigma$ . The effects of the end-to-end stickiness on the looping properties were considered by us recently [35]. In what follows we set  $\epsilon_{\text{s}} = 5k_{\text{B}}T$ .

The dynamics of the position  $\mathbf{r}_i(t)$  of the  $i$ th chain monomer is described by the Langevin equation

$$m \frac{d^2 \mathbf{r}_i(t)}{dt^2} = -\nabla \left[ U_{\text{s}} + \sum_j U_{\text{LJ}}(|\mathbf{r}_i - \mathbf{r}_j|) + U_{\text{b}} \right] - \gamma \frac{d\mathbf{r}_i}{dt} + \boldsymbol{\xi}_i(t). \quad (5)$$

Here  $m$  is the monomer mass,  $\gamma$  is its friction coefficient coupled to the diffusivity via

$$D = k_{\text{B}}T/\gamma \quad (6)$$

and  $\boldsymbol{\xi}_i(t)$  represents a Gaussian white noise source of zero mean with autocorrelation  $\langle \boldsymbol{\xi}_i(t) \cdot \boldsymbol{\xi}_i(t') \rangle = 4\gamma k_{\text{B}}T \delta_{i,i'} \delta(t - t')$ , where  $\delta_{i,i'}$  is the Kronecker delta symbol.

The SPPs are modelled as disks of diameter  $\sigma$  moving under the action of a constant force along a predefined orientation vector

$$\mathbf{n}_j = \left\{ \cos(\theta_j), \sin(\theta_j) \right\}. \quad (7)$$

SPPs interact with each other as well as with polymer monomers via the WCA potential (2), and the position of each SPP is governed by the Langevin equation [27]

$$m \frac{d^2 \mathbf{r}_j(t)}{dt^2} = -\nabla U_{\text{LJ}}(r) + F_{\text{a}} \mathbf{n}_j(t) - \gamma \frac{d\mathbf{r}_j}{dt} + \boldsymbol{\xi}_j(t). \quad (8)$$

Here  $F_{\text{a}}$  is the active force amplitude directly related to the SPP propulsion strength. It can be expressed in terms of the Péclet number  $\text{Pe}$  and the particle velocity  $v$  as

$$\text{Pe} = \frac{v\sigma}{D} = \frac{F_{\text{a}}\sigma}{k_{\text{B}}T}. \quad (9)$$

The orientation  $\theta_j$  of the velocity of the  $j$ th SPP is changing as function of time according to the standard stochastic equation

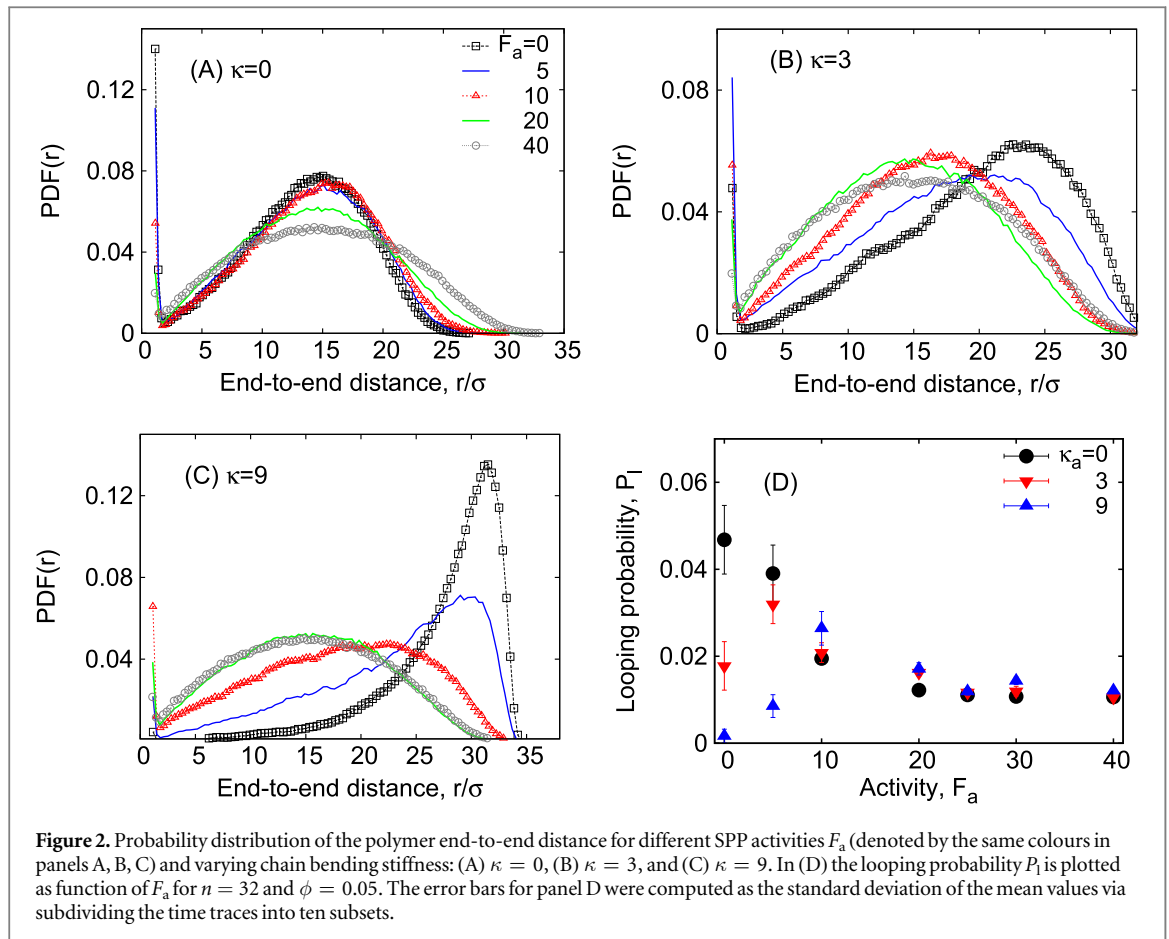
$$\frac{d\theta_j}{dt} = \sqrt{2D_{\text{r}}} \times \xi_{\text{r}}(t). \quad (10)$$

Here  $\xi_{\text{r}}$  is the Gaussian white noise associated with the rotational diffusivity  $D_{\text{r}}$  which satisfies the relation  $D_{\text{r}} = 3D/\sigma^2$  (see, for instance, [27]). Passive particles correspond to  $F_{\text{a}} = 0$ , the situation studied in the context of polymer looping with macromolecular crowding [35].

In our simulations we use periodic boundary conditions for a square box of area  $L^2$  where, depending on the length of the simulated chain,  $L$  varies from 60 to 80 (in units of  $\sigma$ ). The packing fraction of SPPs is defined as

$$\phi = N_{\text{cr}} A_{\text{cr}} / L^2,$$

where  $N_{\text{cr}}$  is the number of SPPs and  $A_{\text{cr}} = \pi(\sigma/2)^2$  is the area of a single SPP. We consider rather dilute SPP systems with  $\phi \leq 0.1$ . For both chain monomers and active particles we choose the unit mass  $m = 1$  and a relatively large friction of  $\gamma = 5$  to ensure a fast momentum relaxation. The time scale in the system is set by the elementary time  $t_0 = \sigma\sqrt{m/(k_{\text{B}}T)}$  [36]; used as the time unit below. We implement the Verlet velocity



algorithm [36] to simulate equations (5) and (8). The integration time step is  $\Delta t = 0.002$ , and we typically run  $\sim 10^{8 \dots 9}$  steps to compute the quantities of interest.

In literature, active Brownian particles were typically studied by simulations in the overdamped limit. The main reason of including the inertia term here is an improved computational efficiency of polymer loop formation. Since the crowder size is the same as that of the polymer monomer, we include the inertia term for them as well. To minimize artifacts of that, we used a relatively high friction coefficient,  $\gamma = 5$ , so that the momentum relaxation time  $t_{rel} = m/\gamma$  remains quite short, about 0.2 (in units of the elementary time  $t_0$ ). The time range for the superdiffusive behaviour we detect in figure 8 below for the monomer and polymer is about 2 ... 5 and 100, respectively (again in terms of  $t_0$ ). Therefore, this superdiffusion stems from the activity of our actively driven particles rather than from their inertial effects.

Generally the activity of SPPs may vary, or some particles in the bath may be completely inactive. To account for this fact, in a part of our study below we consider mixtures of active and inactive particles with respective fractions  $\phi_a$  and  $\phi_i$ . All these particles have the same mass and radius in the simulations.

### 3. Main results

#### 3.1. Polymer dimensions

We first consider the probability distribution function (PDF) of the end to end distance  $r$  of the chain as extracted from long time computer simulations, see figures 2(A)–(C). In our simulations, due to the attraction between the end monomers the standard PDF of the polymer [32] acquires an additional peak around the minimum of the attraction potential at the end to end distance  $r \sim 2^{1/6}\sigma$ . For a flexible chain with  $\kappa = 0$  (figure 2(A)) the chain gets more extended and the peak of the PDF shifts to larger distances when the activity  $F_a$  of SPPs increases. Conversely, for semiflexible chains with a finite value of the polymer stiffness  $\kappa > 0$ , the peak is shifted to shorter distances (figures 2(B) and (C)). These trends are similar to those of [19].

This is the main effect of active particles on the static properties of passive polymer chains in solutions. Inspecting snapshots of the simulations (see also figure 1) or the video files in the supplementary material, one recognizes that active particles effect U or parachute like shapes of the polymer. Such parachute shapes are also observed for membranous red blood cells in cylindrical capillary flows and in blood vessels, see, e.g., [37]. For

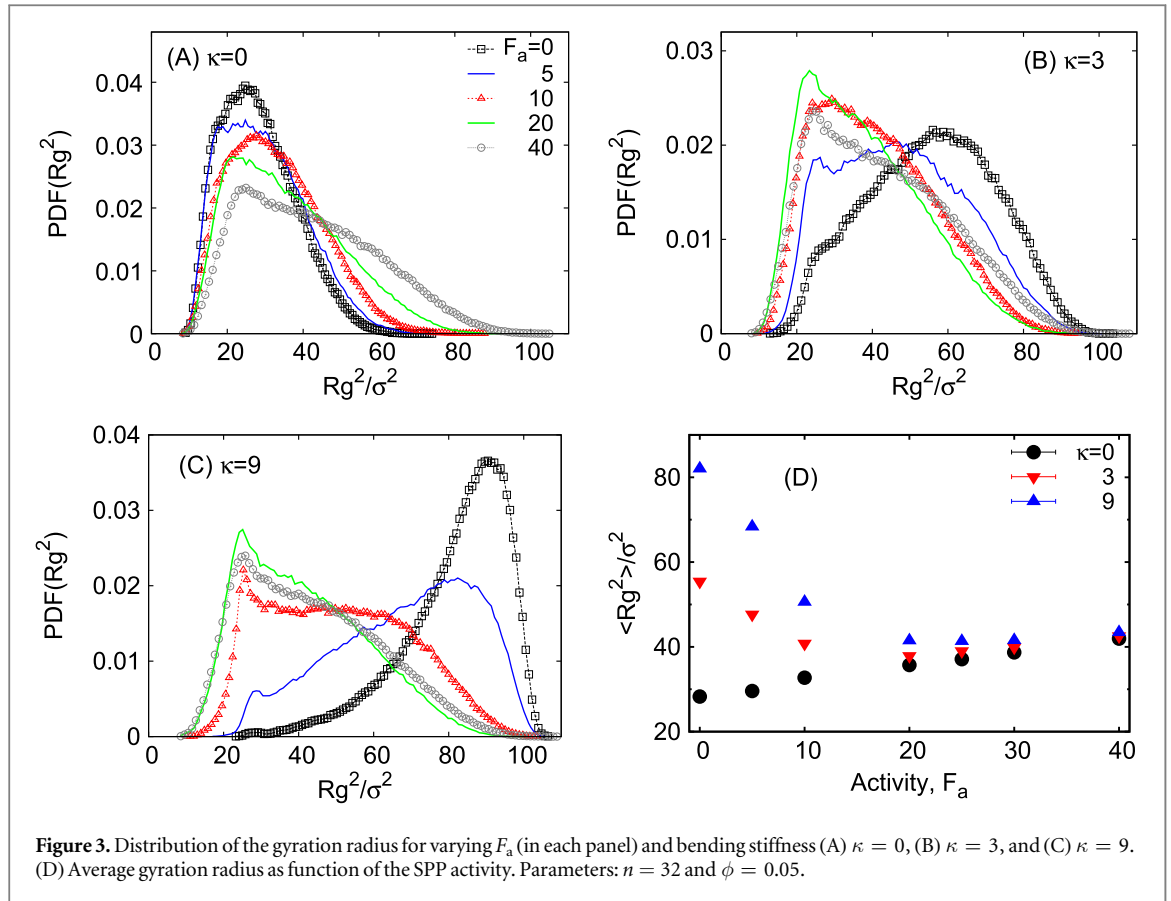


**Figure 3.** Distribution of the gyration radius for varying  $F_a$  (in each panel) and bending stiffness (A)  $\kappa = 0$ , (B)  $\kappa = 3$ , and (C)  $\kappa = 9$ . (D) Average gyration radius as function of the SPP activity. Parameters:  $n = 32$  and  $\phi = 0.05$ .

larger  $F_a$  values—when the SPP forces are much larger than the energetic scale for polymer bending—the looping probability  $P_1$  of the polymer ends is nearly independent on the chain stiffness  $\kappa$ , see figure 2(D).

In figure 3 we also show the distribution of the radius of gyration  $R_g^2$  of the chain and its average value  $\langle R_g^2 \rangle$ . For flexible chains the PDF of the gyration radius broadens towards larger values, causing the monotonic increase of  $\langle R_g^2 \rangle$ . In contrast, for semiflexible chains the gyration radius decreases for  $F_a \leq 20$ , above this value it only slightly increases, compare figure 3(D). This behaviour is consistent with the results of [26, 27].

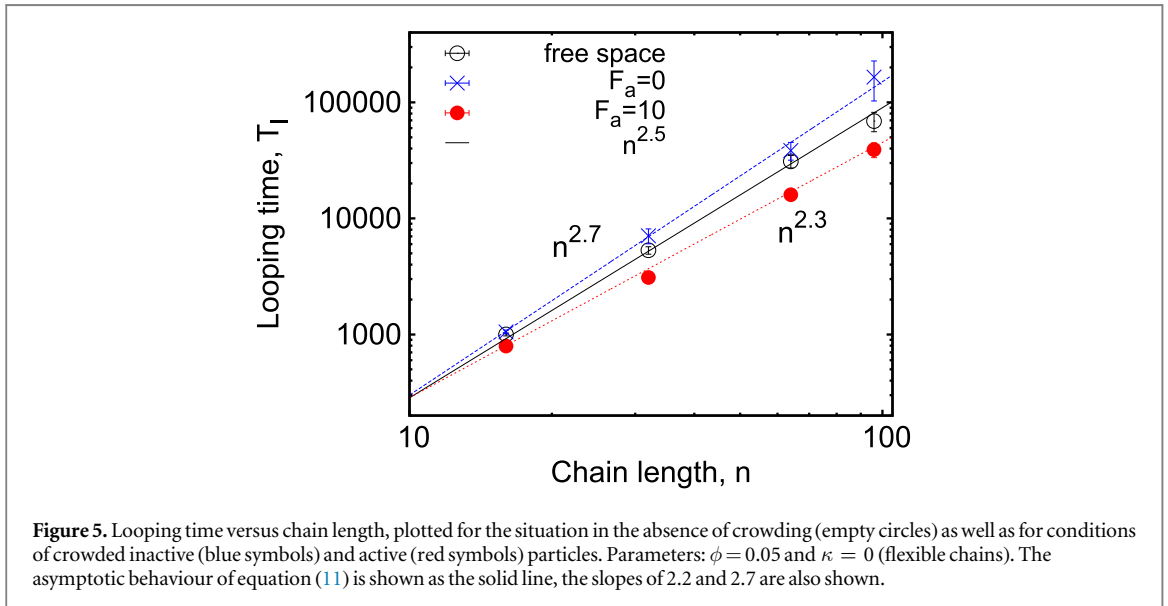
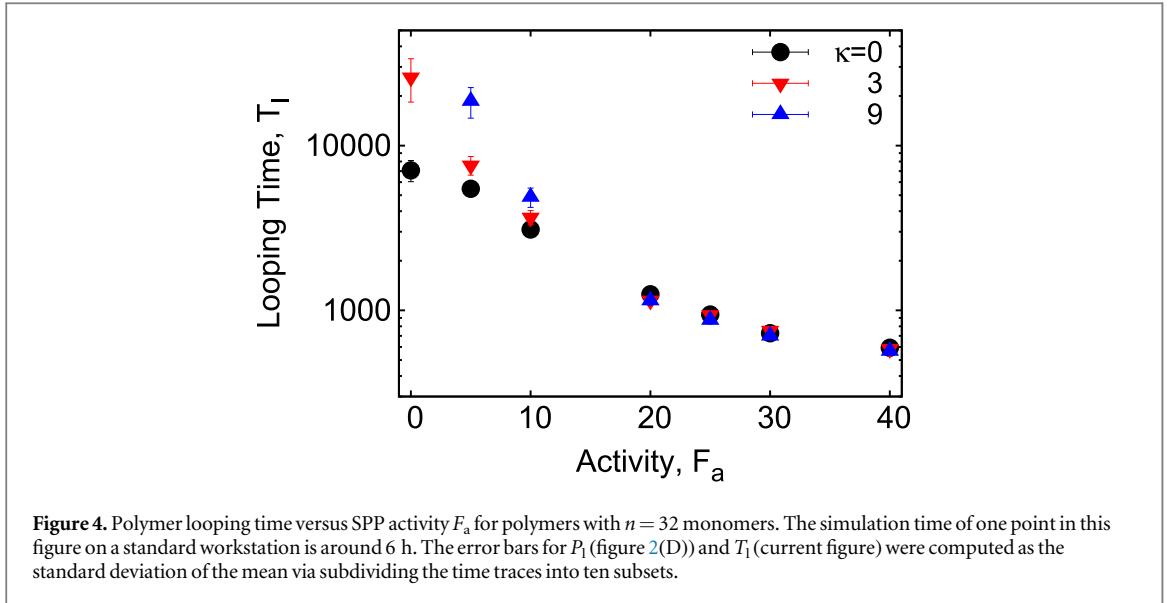
### 3.2. Looping probability and looping time

We observe that the polymer end to end distance shows a highly erratic behaviour as function of time (see also the movies in the Supplementary Material for chains of different flexibility). The polymer ends tend to remain at short distances  $\sim r_c$  due to their attractive energy, while longer end to end distances with  $r \sim r_{eq}$  are favourable entropically at equilibrium. Here  $r_c$  is the so called contact distance, see [35] for details. We compute the looping probability  $P_1$  and the looping time  $T_1$  from the time series of the polymer end to end distance  $|\mathbf{r}_{ee}(t)|$  generated in the simulations. Similar to our recent studies [35, 38] the looping probability  $P_1$  is defined as the fraction of time during which the end to end distance of the chain is shorter than  $r_c$ . In that sense the critical distance  $r_c = 1.75\sigma$  separates the looped and un-looped states of the polymer, compare figures 2(A)–(C).

Figure 2(D) shows the looping probability  $P_1$  as function of the activity  $F_a$  of the SPPs. For flexible chains the value of  $P_1$  decreases monotonically with  $F_a$ . Conversely, for semiflexible polymers the looping probability is non-monotonic in  $F_a$ . This observation indicates two competing effects of the active particles: on the one hand SPPs increase the effective chain flexibility resulting in higher  $P_1$  values. On the other hand, SPPs facilitate the unbinding of end monomers. We observe that, consistent with the shape of the end to end distance PDF at large activity  $F_a$  of SPPs presented in figures 2(A)–(C), for large  $F_a$  the looping probability is almost independent of  $\kappa$ , see figure 2(D).

The polymer looping time  $T_1$  is defined as the time interval within which the distance  $r$  reaches  $r_{eq}$  for the first time and the time it gets shorter than the final distance  $r_f = 1.2\sigma$ , details are shown in figure 3 of [35]. While the distances  $r_c$  and  $r_f$  are mainly determined by the properties of the attractive potential of the end monomers, equation (4), the value of  $r_{eq}$  strongly varies with the chain length and the SPP activity  $F_a$ . From the PDFs of the end to end distances we first determine  $r_{eq}$  for a given chain length  $n\sigma$  and particle activity and then use them to compute the looping time  $T_1$ .

Although the effects of SPPs onto the spatial extension of the immersed polymers were considered previously [26, 27], their dynamic effects—particularly on the polymer end looping reaction—were not



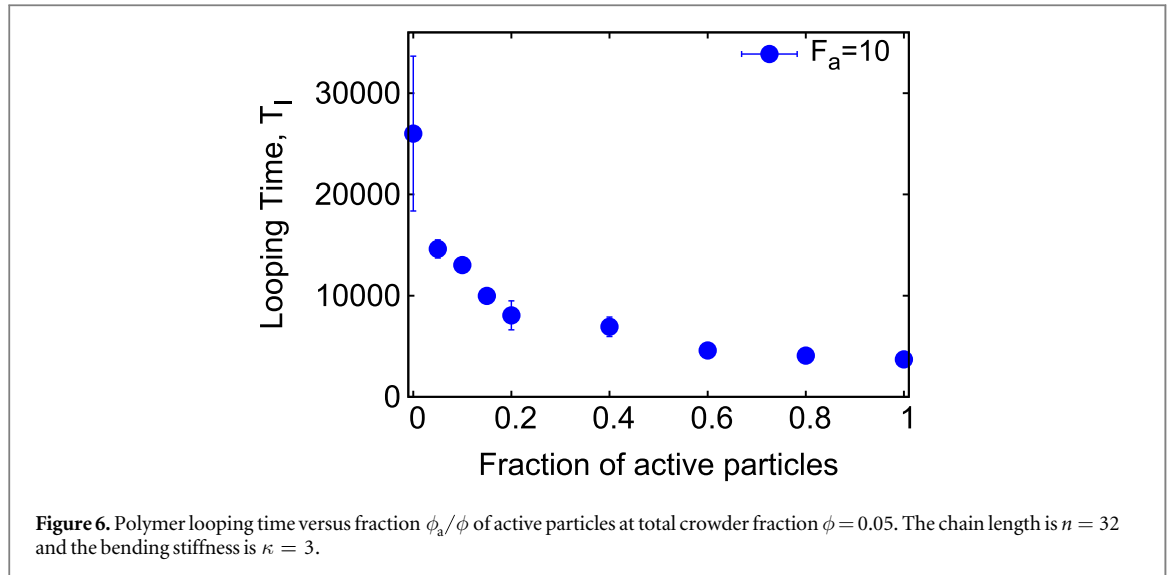
addressed in detail. In figure 4 we present the polymer looping times versus the activity  $F_a$ . In free space or for  $F_a = 0$  the looping takes much longer for stiffer chains because of the large bending energy required for a loop formation. As the SPP activity  $F_a$  increases the polymer looping time decreases, especially for stiff chains: we observe a reduction of  $T_1$  of more than two orders of magnitude, as evidenced in figure 4. Figure 2(D) shows that for large  $F_a$  the looping probability of flexible and semiflexible chains behaves quite similarly, and figure 4 demonstrates similar trends for the looping times  $T_1$  at large SPP activities.

Up to now, we only considered chains with  $n = 32$  monomers. In figure 5 we now show the looping times as a function of the chain length. In free space (i.e. in the absence of crowding,  $\phi = 0$ ), the looping time follows the scaling behaviour [35]

$$T_1(n) \sim n^{2\nu+1}, \quad (11)$$

with the Flory exponent  $\nu = 3/(d + 2) = 3/4$  for a polymer in  $d = 2$  two dimensions. With  $F_a = 0$  (inactive crowders) the looping time increases for a given chain length mainly due to a decreasing monomer diffusivity in the medium [35]. In the presence of active crowders the polymer kinetics becomes facilitated, especially for longer chains, as shown by the red dots in figure 5. Interestingly, in the presence of active particles, the scaling exponent of  $T_1(n)$  decreases somewhat as compared to non-crowded space and passive crowders.

The role of SPPs onto the polymer dynamics is two-fold and the relative contributions depend on the chain stiffness. Namely, active particles enhance the motion of the chain monomers via random collisions. And, when the number of SPPs on both sides of the two-dimensional polymer chain is not the same, the chain starts to crumple. For the case of  $\kappa = 0$ , the polymer is coiled in the absence of SPPs and as their activity increases, the



first effect dominates, thus expanding the polymer (leading to a higher effective temperature). For stiffer chains at  $\kappa > 0$ , the polymer is already expanded and even higher effective temperatures do not perturb it that much (due to high bending energy costs for this). Thus, the second effect becomes more important. In figure 5 we only show the results for flexible chains, because they feature a clear scaling law of the looping time  $T_l$  with the polymer length, in contrast to stiff chains [38]. However, as the activity of SPP increases, the difference in  $T_l$  between the flexible and stiff chains continuously diminishes, as we show in figure 4. In addition, as the polymer length increases, the role of the bending stiffness becomes weaker/secondary. For this reason, the looping time of stiffer chains in the solution of very active SPPs converges to the results for a flexible chain.

In figure 6 we show the polymer looping time versus the relative fraction of active particles,  $\phi_a/\phi$  for the total crowding fraction  $\phi = \phi_a + \phi_i = 0.05$ . We observe that for small values  $\phi_a/\phi$  the magnitude of  $T_l$  initially drops sharply, while the decrease of  $T_l$  for larger fractions of active particles is rather moderate. This indicates that the transition from the non-active to the active results in figure 5 is rather non-uniform/non-linear when active particles are added into the solution.

### 3.3. Tracer diffusion, polymer diffusion and monomer displacements

To get a feeling for the effects of SPPs on the diffusion of passive particles, we now quantify the enhancement of the diffusive motion of a non-active tracer in a bath of SPPs. We track a particle with diameter  $\sigma$  (same size as for the monomers and SPPs) for varying particle activities  $F_a$ . From the time series of the tracer particle position  $\mathbf{r}(t) = \{x(t), y(t)\}$  generated in our simulations we calculate the time averaged mean squared displacement (MSD) [39, 41]

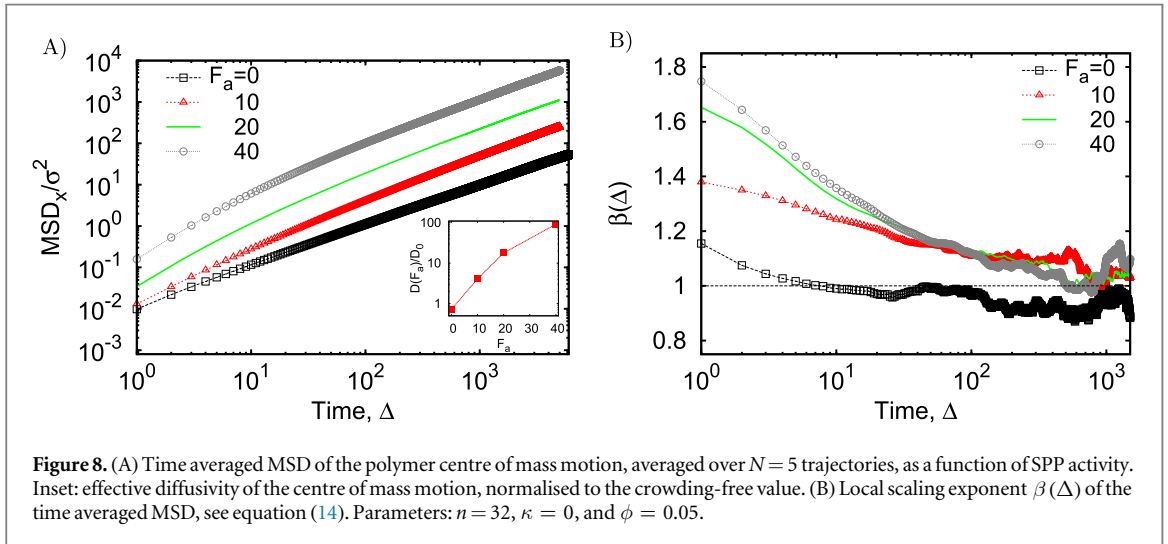
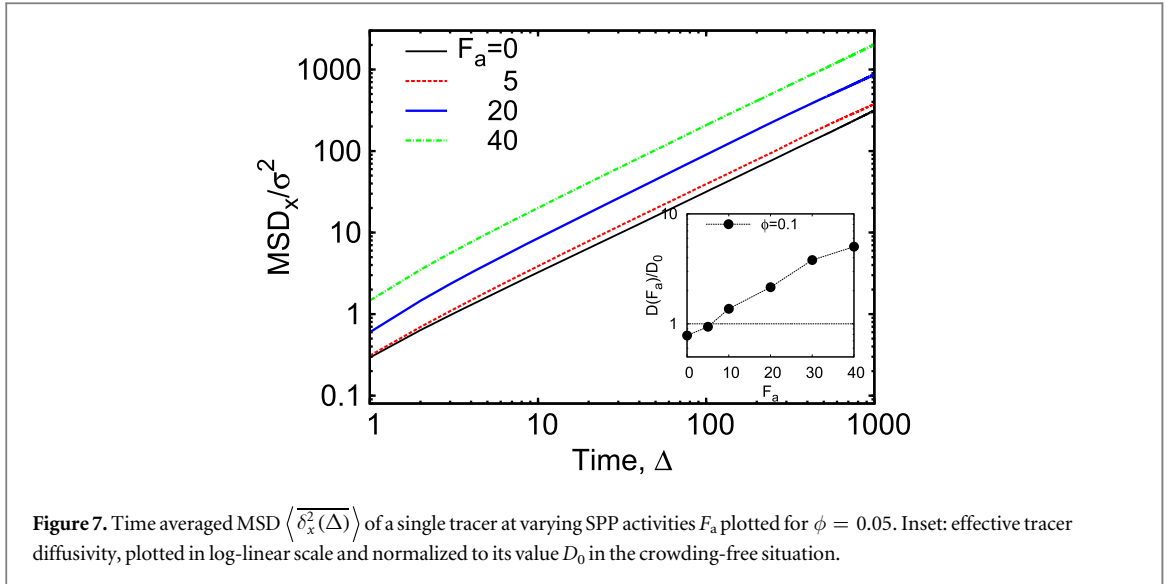
$$\overline{\delta_x^2(\Delta)} = \frac{1}{T - \Delta} \int_0^{T-\Delta} [x(t' + \Delta) - x(t')]^2 dt', \quad (12)$$

where  $\Delta$  is the so called lag time. Here we evaluate the time averaged MSD along the  $x$  coordinate—the results for the  $y$  coordinate are the same. The time averaged MSD is commonly used in single particle tracking analyses of experiments and simulations, when usually few but long  $\mathbf{r}(t)$  traces are available. From a long trace of the particle displacements in space, as recorded in tracking experiments or in computer simulations, one constructs the sliding average via moving the averaging window  $\Delta$  along the trajectory  $\mathbf{r}(t)$  of length  $T$ , according to equation (12). For ergodic processes in the long time limit the ensemble and time averaged MSDs give identical results [39, 40]. In contrast, for many systems featuring anomalous diffusion this is no longer the case and the time averaged MSD provides useful information in addition to the scaling behaviour extracted from the ensemble averaged quantities. The interested reader is referred to the recent review [39] for more details on the time averaged quantities, anomalous diffusion exponents (see also below), and the phenomenon of weak ergodicity breaking. Hereafter, the time averaged MSD is computed with respect to one dimension only. The additional mean

$$\langle \overline{\delta^2(\Delta)} \rangle = \frac{1}{N} \sum_{i=1}^N \overline{\delta_i^2(\Delta)} \quad (13)$$

over an ensemble of  $N$  individual traces  $\overline{\delta_i^2(\Delta)}$  will be analysed below.

We present the time averaged MSD of the tracer particle in figure 7 for varying SPP activity  $F_a$ . The time averaged MSD grows faster than for Brownian motion (superdiffusion [39]) only at very short times,  $\Delta^* \lesssim 2 \dots 5$



(in units of  $t_0$ ), and then turns into the linear Brownian scaling, as expected. Since the momentum relaxation time is shorter than the time scale  $\Delta^*$ , the extended superdiffusion regime is likely due to the impact of active particles.

We extract the diffusivity of the tracer particle through a linear fit to the long time behaviour of the time averaged MSD in the range  $\Delta = 10^2 \dots 10^3$ . As shown in the inset of figure 7 in log-linear scale the diffusivity increases almost exponentially with  $F_a$ . This enhancement is the main reason of the dramatic facilitation of the polymer looping kinetics by highly active particles, as demonstrated in figure 4 as function of the SPP activity  $F_a$ . This is one of the main conclusions of the current paper.

Similarly, in figure 8(A) we show the time averaged MSD of the polymer chain's centre of mass for varying  $F_a$ . Comparison of the magnitudes of the time averaged MSDs shows that, as expected, the centre of mass diffusion of the entire chain is evidently much slower than that of a single tracer particle. In figure 8(B) we compute the local scaling exponent of the time averaged MSD [39, 41]

$$\beta(\Delta) = \frac{d \log \langle \overline{\delta^2}(\Delta) \rangle}{d \log(\Delta)}. \quad (14)$$

We observe that at short time scales the MSD increases superdiffusively with  $\beta > 1$  and the anomalous diffusion exponent grows with increasing  $F_a$  values. At longer times the diffusion exponent decreases and around  $\Delta \simeq 10^3 t_0$  the motion becomes nearly Brownian, albeit with an enhanced diffusivity at higher  $F_a$  values. We expect polymer confinement effects to be much weaker in three dimensions. Therefore, the superdiffusive behaviour of the polymer chain will be less pronounced. On the other hand, the increase of the 'effective

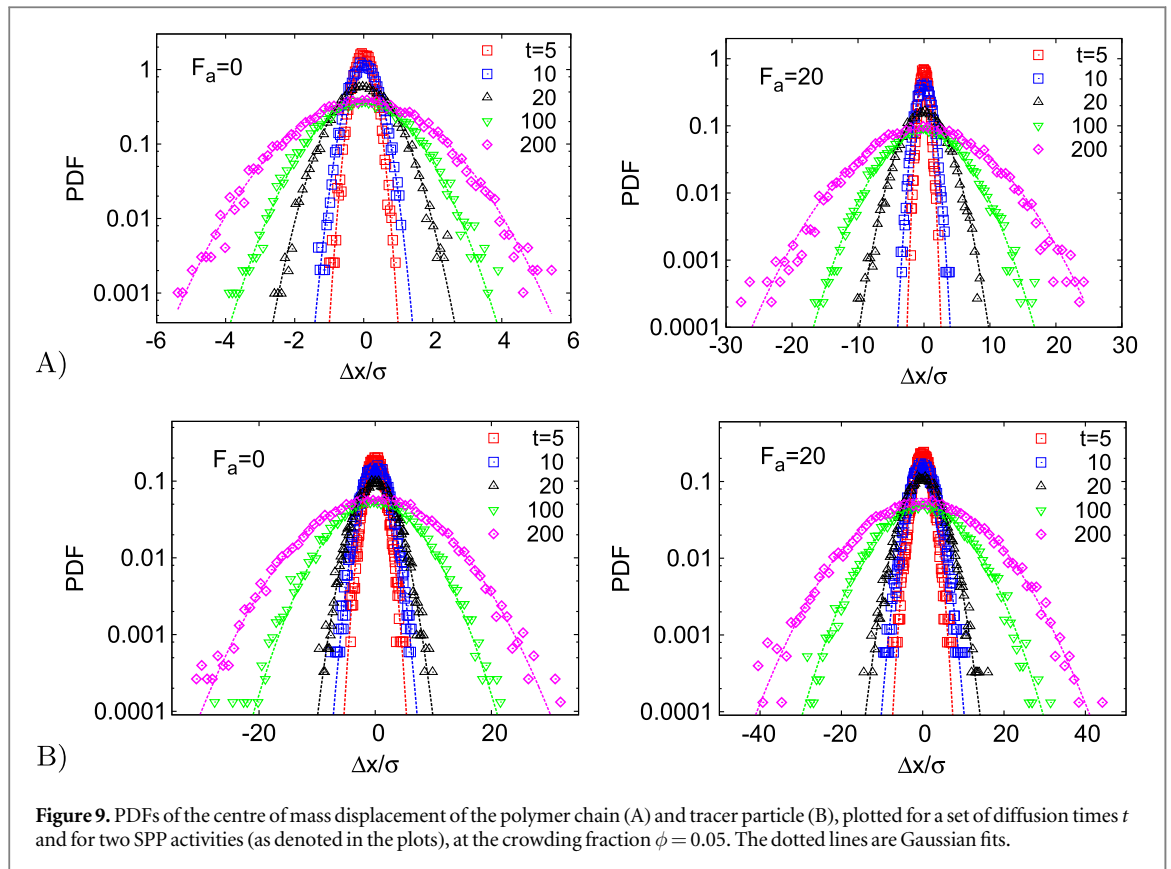


**Figure 9.** PDFs of the centre of mass displacement of the polymer chain (A) and tracer particle (B), plotted for a set of diffusion times  $t$  and for two SPP activities (as denoted in the plots), at the crowding fraction  $\phi = 0.05$ . The dotted lines are Gaussian fits.

temperature' due to collisions with active particles will still exist in the three- dimensional situation, see figure 21 of [35].

In the inset of figure 8(A) we show the chain diffusivity of the centre of mass motion as function of  $F_a$ , normalized with respect to the value in non-crowded space. The diffusivity enhancement is nearly two orders of magnitude, that is much higher than that of a monomeric tracer particle shown in the inset of figure 7. This stronger enhancement is due to pooling of SPPs in the concave region of the parachute-shaped polymer chain, see also the physical mechanism of trapping proposed in [25], resulting in directed motion and faster diffusion of the polymer. This remarkable finding of a giant diffusivity enhancement is our second major result.

We also show the PDFs of the displacement of the polymer and of the tracer particle in panels A and B of figure 9, respectively. Both for active and inactive crowders the PDFs exhibit Gaussian profiles, see the fits in the figure. In the presence of active particles, the width of the corresponding PDF becomes wider, consistent with the enhanced diffusivity picture. This is particularly clear for the polymer centre of mass displacement shown in figure 9(A). Interestingly, even at short times—when the time averaged MSD shows a superdiffusive scaling—the PDFs remain nearly Gaussian (see also [42]).

#### 4. Conclusions

Actively driven systems are inherently out of equilibrium and exhibit peculiar behaviours, for instance, in the ratcheting of motors [43], the formation of living crystals [44, 45], phenomena of ordering [46], mesoscale turbulence phenomena [47], or superfluidic behaviour may be observed in bacterial suspensions [48]. Even elementary laws of thermodynamics may no longer hold [49–51]. In that sense the behaviour of active liquid systems is as rich as that of active soft matter [52].

We studied the dynamics of a polymer chain in a bath of SPPs using Langevin dynamics simulations in two dimensions. We first considered the equilibrium behaviour of the gyration radius, the end to end distance distribution, and the looping probability of the chain as function of the particle activity. We found that a flexible polymer extends monotonically with the SPPs activity. In contrast, for a semiflexible chain—due to a competition of the chain bending and active forces—the polymer size varies non-monotonically with the particle activity. For a larger activity of SPPs—when active forces become dominant over the chain elasticity effects—the extension of both semiflexible and flexible chains behaves quite similarly.

SPPs also significantly impact the polymer kinetics, the main focus of this study. Overall, due to the enhanced diffusivity of the chain monomers, the looping dynamics becomes faster. Especially for the case of stiffer chains the presence of active particles renders the chains effectively softer, and the looping kinetics is dramatically enhanced in comparison to that of flexible chains. Our results indicate that the activity of a cell medium, as mimicked above by active particles, may indeed facilitate DNA loop formation, effectively making the molecule more flexible.

Examining the motion of a tracer particle in the bath of SPPs, in comparison to the motion of the centre of mass of the polymer chain, we observe a giant diffusivity for the driven polymer. We ascribe this to the parachute like shape of the polymer in the SPP bath. Due to the accumulation of SPPs in the concave region of the chain, the polymer performs an extended ballistic motion over long time scales, considerably longer than that of a single monomer. The chain motion at long times becomes Brownian, but with an unexpectedly high renormalized diffusivity. Interestingly, even at time ranges on which the time averaged MSD is superdiffusive, the distribution of the particle displacement remains Gaussian. This result differs from experimental observations of an extended exponential decay of the displacement of a tracer in swimming microorganisms [13]. It would thus be interesting to check whether incorporation of hydrodynamic interactions would reproduce such non-Gaussian behaviour in the model of SPP baths. Moreover, it is an interesting question whether the effect of SPP pooling and the ensuing giant diffusivity enhancement of the polymer motion also arises in three-dimensions.

Clearly, our two-dimensional results without hydrodynamics cannot be applied directly to some realistic mixtures of particles and polymers often immersed in three-dimensional aqueous solutions [1, 5]. The problem is in time-consuming computer simulations involving explicit hydrodynamics. For this, a number of multi-scale computer simulation techniques have been invented in recent years [5, 53], often for supercomputer simulations. Nevertheless we are confident that the main conclusions of the current manuscript—namely, the facilitation of polymer looping and the enhancement of its centre of mass diffusivity with the activity of SPPs—will remain valid also in setups with explicit water, being quantitatively renormalized due to explicit hydrodynamics. On the other hand, the details of the particle displacements e.g. might change due to hydrodynamics. For instance, our Gaussian tracer displacement distributions are different from the experimental findings with stretched tails, see e.g. [15]. Including hydrodynamics could be a direction of our future studies.

Also note that our analysis was performed with an *in vitro* bath of SPPs in mind, but the crowding fraction was chosen to be fairly low. Inside living cells active particles such as molecular motors drive the environment out of equilibrium and fluctuating forces inside cells may indeed become an order of magnitude larger than at the conditions of thermal equilibrium [54]. Concurrently, the metabolic cell activity significantly affects the nature of the cytoplasm and superdiffusive motion may arise [55]. However, the macromolecular crowding fraction in cells typically is of the order of 30...35% [56, 57] and thus exceeds the values of our simulations by far. Moreover, these crowders are quite complex macromolecular objects, which can tune the reaction kinetics stability of biopolymers [58]. It will therefore be interesting to extend our study to higher crowder fractions and different particle geometries, such as star like shapes [59] and polydisperse mixtures of crowders [60].

## Acknowledgments

We acknowledge funding from the Academy of Finland (Suomen Akatemia, Finland Distinguished Professorship to RM) and the Deutsche Forschungsgemeinschaft (DFG Grant to AGC).

## References

- [1] Romanczuk P, Bär M, Ebeling W, Lindner B and Schimansky-Geier L 2012 *Eur. Phys. J. Spec. Top.* **202** 1 and references therein
- [2] Marchetti M C, Joanny J F, Ramaswamy S, Liverpool T B, Prost J, Rao M and Simha R A 2013 *Rev. Mod. Phys.* **85** 1143
- [3] Jülicher F, Ajdari A and Prost J 1997 *Rev. Mod. Phys.* **69** 1269  
Kolomeisky A B and Fisher M E 2007 *Ann. Rev. Phys. Chem.* **58** 675  
Astumian R D and Hänggi P 2002 *Phys. Today* **55** 33
- [4] Robert D, Nguyen T H, Gallet F and Wilhelm C 2010 *PLoS One* **4** e10046  
Goychuk I, Kharchenko V O and Metzler R 2014 *PLoS One* **9** e91700  
Goychuk I, Kharchenko V O and Metzler R 2014 *Phys. Chem. Chem. Phys.* **16** 16524
- [5] Elgeti J, Winkler R G and Gompper G 2015 *Rep. Prog. Phys.* **78** 056601 and references therein
- [6] Cates M E 2012 *Rep. Prog. Phys.* **75** 042601
- [7] Karamouzias I, Skinner B and Guy S J 2014 *Phys. Rev. Lett.* **113** 238701  
Brockmann D, Hufnagel L and Geisel T 2006 *Nature* **439** 462  
Bénichou O, Loverdo C, Moreau M and Voituriez R 2011 *Rev. Mod. Phys.* **83** 81  
Bresloff P C and Newby J M 2013 *Rev. Mod. Phys.* **85** 135  
Song C, Koren T, Wang P and Barabási A L 2010 *Nat. Phys.* **6** 818

- [8] Howse J R, Jones R A L, Ryan A J, Gough T, Vafabakhsh R and Golestanian R 2007 *Phys. Rev. Lett.* **99** 048102  
Paxton W F *et al* 2006 *J. Am. Chem. Soc.* **128** 14881  
Palacci J, Cottin-Bizonne C, Ybert C and Bocquet L 2010 *Phys. Rev. Lett.* **105** 088304
- [9] Jiang H-R, Yoshinaga N and Sano M 2010 *Phys. Rev. Lett.* **105** 268302
- [10] Hänggi P and Marchesoni F 2009 *Rev. Mod. Phys.* **81** 387  
Ghosh P K, Hänggi P, Marchesoni F and Nori F 2014 *Phys. Rev. E* **89** 062115
- [11] Loverdo C, Bénichou O, Moreau M and Voituriez R 2008 *Nat. Phys.* **9** 134  
Loverdo C, Bénichou O, Moreau M and Voituriez R 2009 *J. Stat. Mech.* **P02045**  
Godec A and Metzler R 2015 *Phys. Rev. E* **92** 010701 (R)  
Chen K, Wang B and Granick S 2015 *Nat. Mater.* **14** 589
- [12] Viswanathan G M, da Luz M G E, Raposo E P and Stanley H E 2011 *The Physics of Foraging: An Introduction to Random Searches and Biological Encounters* (New York: Cambridge University Press)  
Lomholt M A, Koren T, Metzler R and Klafter J 2008 *Proc. Natl Acad. Sci. USA* **105** 11055  
Palyulin V V, Chechkin A V and Metzler R 2014 *Proc. Natl Acad. Sci. USA* **111** 2931  
Sims D W *et al* 2008 *Nature* **451** 1098
- [13] Wu X-L and Libchaber A 2000 *Phys. Rev. Lett.* **84** 3017
- [14] Jepsen A, Martinez V A, Schwarz-Linek J, Morozov A and Poon W C K 2013 *Phys. Rev. E* **88** 041002 (R)
- [15] Leptos K C, Guasto J S, Gollub J P, Pesci A I and Goldstein R E 2009 *Phys. Rev. Lett.* **103** 198103
- [16] Morozov A and Marenduzzo D 2014 *Soft Matter* **10** 2748
- [17] Mussel M, Zeevy K, Diamant H and Nevo U 2014 *Biophys. J.* **106** 2710  
Roy S *et al* 2007 *J. Neurosci.* **27** 3131  
Scott D A *et al* 2011 *Neuron* **70** 441
- [18] Asakura S and Oosawa F 1954 *J. Chem. Phys.* **22** 1255
- [19] Harder J, Mallory S A, Tung C, Valeriani C and Cacciuto A 2014 *J. Chem. Phys.* **141** 194901
- [20] Ni R, Cohen Stuart M A and Bolhuis P G 2015 *Phys. Rev. Lett.* **114** 018302
- [21] Elgeti J and Gompper G 2013 *Europhys. Lett.* **101** 48003
- [22] Matas-Navarro R, Golestanian R, Liverpool T B and Fielding S M 2014 *Phys. Rev. E* **90** 032304  
Navarro R M and Fielding S 2015 *Soft Matter* **11** 7525 and references cited therein
- [23] Peruani F and Sibona G J 2008 *Phys. Rev. Lett.* **100** 168103
- [24] Fily Y and Marchetti M C 2012 *Phys. Rev. Lett.* **108** 235702
- [25] Chepizhko O and Peruani F 2013 *Phys. Rev. Lett.* **111** 160604
- [26] Kaiser A and Löwen H 2014 *J. Chem. Phys.* **141** 044903
- [27] Harder J, Valeriani C and Cacciuto A 2014 *Phys. Rev. E* **90** 062312
- [28] Schleif R 1992 *Annu. Rev. Biochem.* **61** 199
- [29] Matthews K S 1992 *Microbiology Mol. Biol. Rev.* **56** 123
- [30] Tan C, Saurabh S, Bruchez M P, Schwartz R and LeDuc P 2013 *Nat. Nanotechnology* **8** 602  
Vilar J M G and Saiz I 2013 *ACS Synth. Biol.* **2** 576
- [31] van den Broek B, Lomholt M A, Kalisch S-M J, Metzler R and Wuite G J L 2008 *Proc. Natl Acad. Sci. USA* **105** 15738  
Lomholt M A, Broek B v d, Kalisch S-M J, Wuite G J L and Metzler R 2009 *Proc. Natl Acad. Sci. USA* **106** 8204  
Bauer M, Rasmussen E S, Lomholt M A and Metzler R 2015 *Sci. Rep.* **5** 10072  
Swigon D, Coleman B D and Olson W K 2006 *Proc. Natl Acad. Sci. USA* **103** 9879  
Amitai A and Holcman D 2013 *Phys. Rev. Lett.* **110** 248105
- [32] Cherstvy A G 2011 *Eur. Biophys. J.* **40** 69  
Cherstvy A G 2011 *J. Phys. Chem. B* **115** 4286
- [33] Tyagi S and Kramer F R 1996 *Nat. Biotechnology* **14** 303  
Bonnet G, Krichesky O and Libchaber A 1998 *Proc. Natl Acad. Sci. USA* **95** 8602
- [34] Stiehl O, Weidner-Hertrampf K and Weiss M 2013 *New J. Phys.* **15** 113010
- [35] Shin J, Cherstvy A G and Metzler R 2015 *Soft Matter* **11** 472
- [36] Allen M P and Tildesley D J 1994 *Computer Simulation of Liquids* (Oxford: Clarendon)
- [37] Noguchi H and Gompper G 2005 *Proc. Natl Acad. Sci. USA* **102** 14159
- [38] Shin J, Cherstvy A G and Metzler R 2015 *ACS Macro Lett.* **4** 202
- [39] Metzler R, Jeon J-H, Cherstvy A G and Barkai E 2014 *Phys. Chem. Chem. Phys.* **16** 24128
- [40] Ghosh S K, Cherstvy A G and Metzler R 2015 *Phys. Chem. Chem. Phys.* **17** 1847
- [41] Höfling F and Franosch T 2013 *Rep. Prog. Phys.* **76** 046602
- [42] Wang B, Kuo J, Bae S C and Granick S 2012 *Nat. Mater.* **11** 481
- [43] Di Leonardo R *et al* 2010 *Proc. Natl Acad. Sci. USA* **107** 9541
- [44] Palacci J, Sacanna S, Steinberg A F, Pine D J and Chaikin P M 2013 *Science* **339** 936
- [45] Buttinoni I, Bialke J, Kuemmel F, Löwen H, Bechinger C and Speck T 2013 *Phys. Rev. Lett.* **110** 238301
- [46] Hennes M, Wolff K and Stark H 2014 *Phys. Rev. Lett.* **112** 238104
- [47] Wensink H H, Dunkel J, Heidenreich S, Drescher K, Goldstein R E, Löwen H and Yeomans J M 2012 *Proc. Natl Acad. Sci. USA* **109** 14308
- [48] López H M, Gachelin J, Douarce C, Auradou H and Clément E 2015 *Phys. Rev. Lett.* **115** 028301
- [49] Mallory S A, Saric A, Valeriani C and Cacciuto A 2014 *Phys. Rev. E* **89** 052303
- [50] Solon A P, Fily Y, Baskaran A, Cates M E, Kafri Y, Kardar M and Tailleur J 2015 *Nat. Phys.* **11** 673
- [51] Solon A P, Stenhammar J, Wittkowski R, Kardar M, Kafri Y, Cates M E and Tailleur J 2015 *Phys. Rev. Lett.* **114** 198301
- [52] Menzel A M 2015 *Phys. Rep.* **554** 1
- [53] Gompper G, Ihle T, Kroll D M and Winkler R G 2008 *Adv. Polym. Sci.* **221** 1
- [54] Gallet F, Arcizet D, Bohec P and Richert A 2009 *Soft Matter* **5** 2947
- [55] Parry B R, Surovtsev I V, Cabeen M T, O'Hern C S, Dufresne E R and Jacobs-Wagner C 2014 *Cell* **156** 183  
Reverey J F, Jeon J H, Bao H, Leippe M, Metzler R and Selhuber-Unkel C 2015 *Sci. Rep.* **5** 11690
- [56] Zimmerman S B and Minton A P 1993 *Annu. Rev. Biophys. Biomol. Struct.* **22** 27
- [57] McGuffee A R and Elcock A H 2010 *PLoS Comput. Biol.* **6** e1000694

- [58] Kang H, Pincus P A, Hyeon C and Thirumalai D 2015 *Phys. Rev. Lett.* **114** 068303  
Zhou H X, Rivas G and Minton A P 2008 *Ann. Rev. Biophys.* **37** 375  
Denesyuk N A and Thirumalai D 2011 *J. Am. Chem. Soc.* **133** 11858  
Toan N M, Marenduzzo D, Cook P R and Micheletti C 2006 *Phys. Rev. Lett.* **97** 178302  
Minton A P 2000 *Curr. Opin. Struct. Biol.* **10** 34  
Yanagisawa M, Sakaue T and Yoshikawa K 2014 *Int. Rev. Cell & Mol. Biol.* **307** 175  
Denton A R 2014 *Int. Rev. Cell & Mol. Biol.* **307** 27
- [59] Shin J, Cherstvy A G and Metzler R 2015 *New J. Phys.* accepted
- [60] Kondrat S, Zimmermann O, Wiechert W and von Lieres E 2015 *Phys. Biol.* **12** 046003